NUMERICAL METHOD FOR SAINT -VENANT TORSION PROBLEM WITH ARBITRARY CROSS- SECTIONS

Dang-Bao TRAN[1,3], Jaroslav NAVRÁTIL[1], Martin ČERMÁK[2]

[1] Department of Structures, Faculty of Civil Engineering, VSB – Technical University of Ostrava, Ludvíka Podéště 1875/17, 708 00 Ostrava-Poruba, Czech Republic
[2] Department of Mathematics, Faculty of Civil Engineering, VSB – Technical University of Ostrava, Ludvíka Podéště 1875/17, 708 00 Ostrava-Poruba, Czech Republic
[3] Department of Civil Engineering, Faculty of Architecture, Thu Dau Mot University, Tran Van On 06, Binh Duong Province, Vietnam

jaroslav.navratil@vsb.cz, martin.cermak@vsb.cz, dang.bao.tran.st@vsb.cz, baotd@tdmu.edu.vn

Abstract. *A numerical method solving the Saint-Venant torsion problem with arbitrary cross-sections was derived by Gruttmann in 1999. The numerical method is validated by analyzing two examples with two mesh types: uniform and non-uniform; excellent accuracy was obtained compared to analytical solutions. Further, the comparison between three elements: LINQUAD, QUAD8NOD, and QUAD9NOD to choose the appropriate element for the numerical method was performed. The conclusion drawn is that our numerical method with QUAD8NOD and QUAD9NOD elements is suitable for Saint-Venant torsion problem.*

Keywords

Gruttmann shear stress, Saint-Venant torsion, Quadrilateral element type.

1.   Introduction

The Saint-Venant problem of torsion is a classical problem that was described in detail on the theory of elasticity [1]. Numerical analysis of the torsion problem using the finite element method has been demonstrated by many researchers. Gruttmann [2] described the solution with the use of warping function, which is more attractive than Prandtl's stress function, because in this case, the continuity conditions around the holes of a multiple connected domain are automatically fulfilled.

The objectives of the paper are summarized as follows: i) to present and assess our numerical method to solve the Saint-Venant torsion problem derived from the results of Gruttmann with the theory analytical, ii) to compare three

types of quadrilateral elements: Four-node linear quadrilateral element denoted as *LINQUAD*, Eight-node quadrilateral element denoted as *QUAD8NOD*, Nine-node quadrilateral element denoted as *QUAD9NOD* in order to choose the appropriate element for our numerical method.

2.   Solution procedure by numerical method

Gruttmann [2] considers a prismatic bar, whose longitudinal axis is the x–axis, and whose cross–sections lie in the y–z–plane, see Fig. 1. The considered domain Ω with boundary $\partial\Omega$ may be multiple connected. On $\partial\Omega$ the right- handed orthogonal basis system is defined with tangent vector t and outward normal vector $\mathbf{n} = [n_y, n_z]^T$. With t the orientation of the associated coordinate s is uniquely defined.
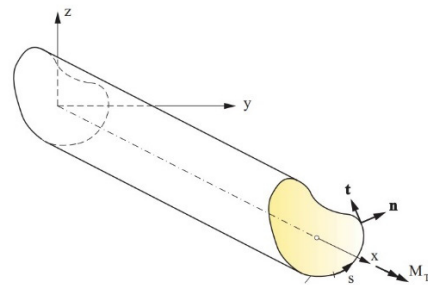

Fig. 1:   Torsion of a prismatic beam [2]

Assuming the invariable cross-section, the homogeneous isotropic elastic material. The displacement field of prsimatic beam $\mathbf{u} = [u_x, u_y, u_z]^T$ is given by

$$u_x = \alpha \omega^T , \ u_y = -\beta_x z , \ u_z = -\beta_x y, \tag{1}$$

where β_x: torsion angle, $\alpha = \dfrac{d\beta_x}{dx}$, $\omega^T(y,z)$: warping function for torsion. Here, the constraint is required

$$\int_\Omega \omega^T \, dA = 0 . \tag{2}$$

The shear stresses are defined by

$$\tau_{xy} = G\alpha\left(\frac{\partial \omega^T}{\partial y} - z\right), \ \tau_{xz} = G\alpha\left(\frac{\partial \omega^T}{\partial z} + y\right), \tag{3}$$

where G is shear modulus.

The polar second moment of area of the shaft cross-section can read as

$$I_T = \int_\Omega \left[\left(\frac{\partial \omega^T}{\partial z} + y\right)y - \left(\frac{\partial \omega^T}{\partial y} - z\right)z\right]dA. \tag{4}$$

The strong form of the boundary value problem is described by

$$\frac{\partial^2 \omega^T}{\partial^2 y} + \frac{\partial^2 \omega^T}{\partial^2 z} = 0 \ \ in \ \Omega,$$

$$n_y \frac{\partial \omega^T}{\partial y} + n_z \frac{\partial \omega^T}{\partial z} = n_y z - n_z y \ \ on \ \partial\Omega. \tag{5}$$

$$n_y = \frac{dz}{ds} , \ n_z = -\frac{dy}{ds}. \tag{6}$$

Using the Galerkin's method, with test function $\eta \in V$ with $V = \{\eta \in H^1(\Omega), \eta = 0 \ on \ \partial\Omega_{\omega^T}\}$, Gruttmann [2] transformed the strong form (5) to the weak form as below

$$G(\omega^T,\eta) = 0,$$

$$\int_\Omega \left[\frac{\partial \omega^T}{\partial y}\frac{\partial \eta}{\partial y} + \frac{\partial \omega^T}{\partial z}\frac{\partial \eta}{\partial z}\right]dA - \iint_{\partial\Omega}(n_y z - n_z y)\eta \, ds = 0. \tag{7}$$

The weak form of the boundary value problem (7) can be solved approximately using the finite element method. Using the isoparametric formulation, the $\mathbf{x} = [y,z]^T$, the unknown function ω^T and the test function η are interpolated within a typical element using the same shape functions

$$\mathbf{x}^h = \sum_{i=1}^{nel} N_I(\xi,\eta)\mathbf{x}_i, \ (\omega^T)^h = \sum_{i=1}^{nel} N_I(\xi,\eta)\omega_i^T,$$

$$(\eta)^h = \sum_{i=1}^{nel} N_I(\xi,\eta)\eta_i, \tag{8}$$

where *nel* denotes the number of nodes per element. The index *h* is used to denote the approximate solution of the finite element method.

The shape functions $N_I(\xi,\eta)$ of reference element for *LINQUAD, QUAD8NOD, QUAD9NOD,* which were used in our numerical method, are introduced in Appendix A. For more detail, we refer e.g. to [3], [4].

Inserting the derivatives of $(\omega^T)^h$ and η^h into the weak form (7) yields the finite element equation

$$\bigcup_{e=1}^{numel} \sum_{I=1}^{nel} \sum_{K=1}^{nel} \delta\omega_I^T (K_{IK}^e \omega_K^T - F_I^e) = 0. \tag{9}$$

The operator $\bigcup$ describes the assembly and *numel* the total number of finite elements to solve the problem. The stiffness part K_{IK}^e to the nodes *I* and *K* as well as the right hand F_I^e yields

$$K_{IK}^e = \int_{\Omega_e}\left(\frac{\partial N_I}{\partial y}\frac{\partial N_K}{\partial y} + \frac{\partial N_I}{\partial z}\frac{\partial N_K}{\partial z}\right)dA_e = \int_{-1}^{1}\int_{-1}^{1}\left(\frac{\partial N_I}{\partial y}\frac{\partial N_K}{\partial y} + \frac{\partial N_I}{\partial z}\frac{\partial N_K}{\partial z}\right)|\mathbf{J}|\,d\xi d\eta,$$

$$K_{IK}^e = \sum_{p=1}^{P}\sum_{q=1}^{Q} w_p w_q \left(\frac{\partial N_I}{\partial y}(\xi_p,\eta_q)\frac{\partial N_K}{\partial y}(\xi_p,\eta_q) + \frac{\partial N_I}{\partial z}(\xi_p,\eta_q)\frac{\partial N_K}{\partial z}(\xi_p,\eta_q)\right)|\mathbf{J}(\xi_p,\eta_q)|, \tag{10}$$

$$F_I^e = \int_{\Omega_e}\left(\frac{\partial N_I}{\partial y}z - \frac{\partial N_I}{\partial z}y\right)dA_e = \int_{-1}^{1}\int_{-1}^{1}\left(\frac{\partial N_I}{\partial y}z + \frac{\partial N_I}{\partial z}y\right)|\mathbf{J}|\,d\xi d\eta,$$

$$F_I^e = \sum_{p=1}^{P}\sum_{q=1}^{Q} w_p w_q \left(\frac{\partial N_I}{\partial y}(\xi_p,\eta_q)z - \frac{\partial N_I}{\partial z}(\xi_p,\eta_q)y\right)|\mathbf{J}(\xi_p,\eta_q)|, \tag{11}$$

in which $\mathbf{J}$ denoted as Jacobian matrix defined as

$$\mathbf{J} = \begin{bmatrix} \dfrac{\partial y}{\partial x} & \dfrac{\partial z}{\partial h} \\ \dfrac{\partial y}{\partial x} & \dfrac{\partial z}{\partial h} \end{bmatrix} \tag{12}$$

w_p and w_q are the weights and ξ_p and η_q are the integration points of the Gaussian integration technique. For *LINQUAD* reference element, we use 2 x 2 Gauss quadrature derived from the 1D case where the quadrature points are located at $-1/\sqrt{3}$ and $1/\sqrt{3}$, and the corresponding weights are equal to 1 and 1, respectively (see [3]).

For *QUAD8NOD, QUAD9NOD* reference element, we use 3 x 3 Gauss quadrature derived from the 1D case,

where the quadrature points are located at $-\sqrt{3/5}$, 0 and $\sqrt{3/5}$, and the corresponding weights are equal to 5/9, 8/9, and 5/9, respectively (see [3]).

The value ω_I^T of one arbitrary nodal point I has to be value 0.

3. Verification examples

Verification examples were implemented by MATLAB R2015a on a personal computer with Intel(R) Core(TM) i5-8265U CPU @ 1.60GHz (8 CPUs), ~1.8GHz , 16 GB RAM, and 500 GB hard disk memory. Calculation times are given in seconds.

We consider two Saint-Venant torsion examples presented in Theory of Elasticity [1]. The first example is a bar of square cross-section subjected to the torsion moment $M = 1$ [MN.m] with the length of the edge 1 m. The values of maximum shear stress and torsional moment of inertia obtained by analytical solution [1] are $\tau_{max} = 4.80769$ [MPa], $I_T = 0.1406$ [m^4].

An equilateral triangle under torsion moment $M = 1$ [kN.m] will be analyzed in the second example. The height of the triangle is 200 mm. The results of maximum shear stress τ_{max} and torsional moment of inertia I_T are 1.62380 [MPa] and 6158.40 [cm^4] respectively.

We divided 4, 16, 64, 256, 1024, 4096, 16384, 65536 elements for square section and 3,12, 37, 57, 109, 661, 896, 1578 elements for triangular section. With these investigated models, we found the value of maximum shear stress, the moment of inertia, and the computation times of each element.

4. Results

It is clear from Table 1, Table 2 that the results of the maximum shear stress, the torsional moment of inertia obtained from our numerical method are in good agreement with the theoretical solution. It is remarkable that we performed two examples with two different ways of meshing: uniform mesh see Fig.2(a) and non-uniform mesh see Fig.2(b) to check the accuracy of numerical method.

Fig.3 shows the computation times of *LINQUAD* is better than *QUAD8NOD* and *QUAD9NOD* in the same discrete size. If the last results are considered, the computation times of *QUAD8NOD* and *QUAD9NOD* will be better than *LINQUAD*, see Table 1, Table 2.

It is noticeable from Fig.4 and Fig.5 that the values of the maximum shear stress, the moment of inertia obtained by *QUAD8NOD* and *QUAD9NOD* decrease to the analytical values when the number of elements increase.

This is the opposite when *LINQUAD* is used. It means when *QUAD8NOD* and *QUAD9NOD* is used, the results are enough safe in the design of structures although the element is not meshed fine enough. We can also see that the convergence speed of *QUAD8NOD* and *QUAD9NO*D is faster than *LINQUAD*.

Tab. 1: Square section in torsion

Factors	Element type		
	LINQUAD	*QUAD8NODE*	*QUAD9NODE*
Number of elements	65536	256	256
Number of nodes	66049	833	1089
τ_{max} [a][MPa]	4.80377	4.81169	4.81162
I_T [b][m^4]	0.14058	0.14058	0.14058
Times [s]	620	2.4	2.5
Error [a], %	0.082	0.083	0.082
Error [b],%	0.015	0.016	0.016

Tab. 2: Triangular section in torsion

Factors	Element type		
	LINQUAD	*QUAD8NODE*	*QUAD9NODE*
Number of elements	1578	661	661
Number of Nodes	1669	2092	2753
τ_{max} [a][MPa]	1.62253	1.62452	1.62462
I_T [b][cm^4]	6161.24	6158.4	6158.4
Times [s]	6.0	4.9	4.9
Error [a],%	0.078	0.045	0.051
Error [b],%	0.046	0.00	0.000

The phenomenon that the cross- section of the bar does not remain in the plane during torsion is presented in Fig.6. The maximum shear stress corresponding to the maximum slope of the membrane is at the middle points of the long sides of the rectangle [1]. It means the distribution of shear stress of the square section decreases from middle point of edge to the center. Fig.7 shows a good agreement with the theoretical results.

From [1] the stress τ_{xz} get the maximum value in the middle of the sides of the triangle and the zero value in the center of the triangle. It is quite clear in Fig.6.

5. Conclusions

In this paper, we have studied how to derive the numerical method from Gruttmann's paper [2] to solve the Saint-Venant problem of torsion with arbitrary cross-section. The verification of the numerical method has been carried out by analyzing two examples with two different mesh

types: uniform and non-uniform. The comparison of the factors as the mesh size, the computation times to choose the appropriate element for our numerical method was performed. The study has shown (i) an excellent agreement of the results of our numerical method with the analytical method, (ii) *QUAD8NOD* and *QUAD9NOD* element are the appropriate elements for our numerical method.
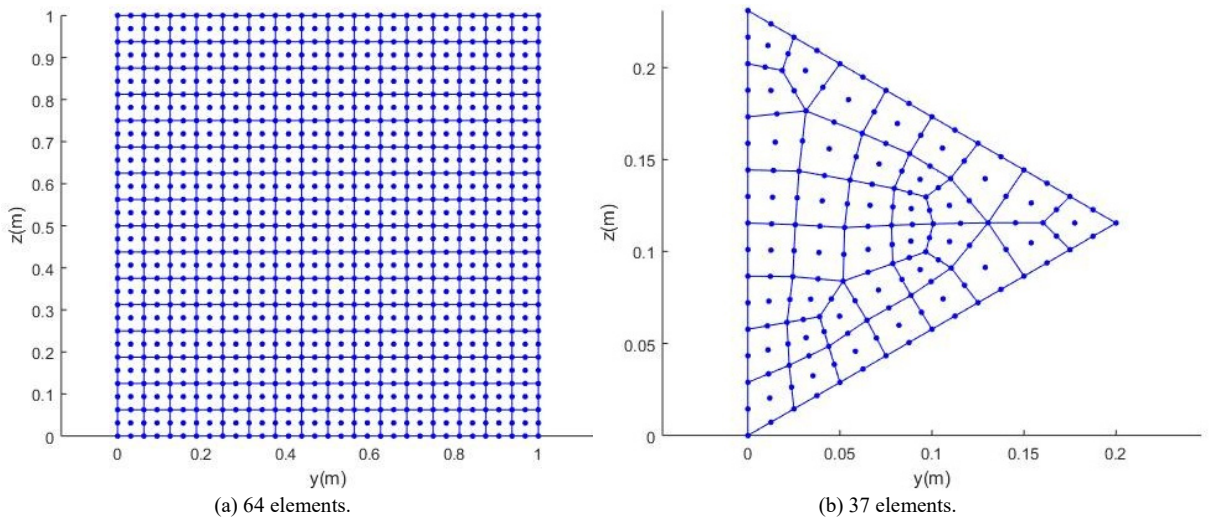

(a) 64 elements.   (b) 37 elements.

Fig. 2: The mesh typical with *QUAD9NOD* for square section with (a) 64 elements and triangular section with (b) 37elements.

(a) square section.   (b) triangular section.

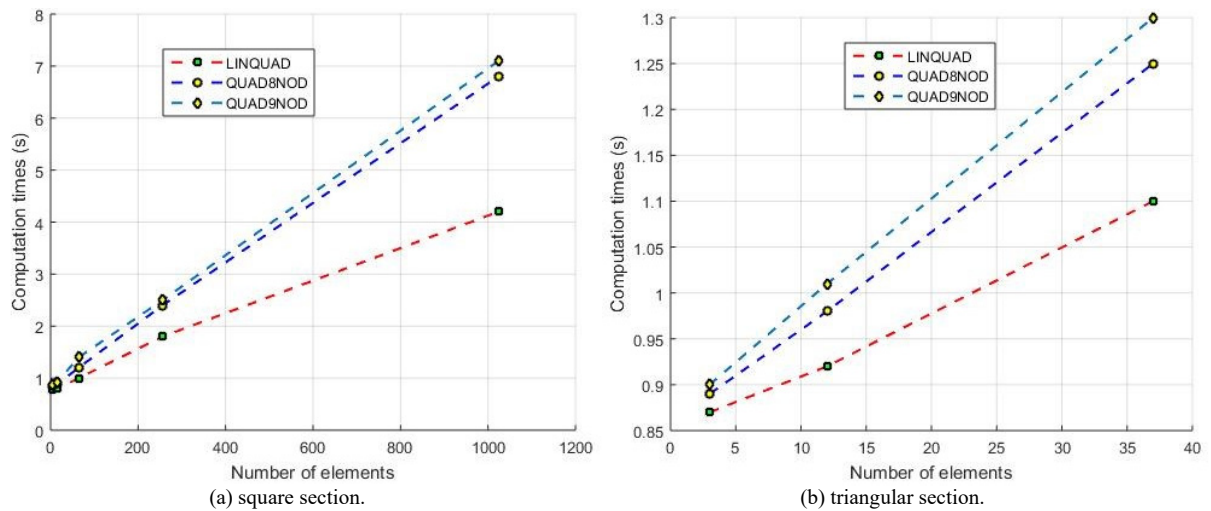**Fig. 3:** The computation time of three elements with respect to the number of elements for (a) square section and (b) triangular section.

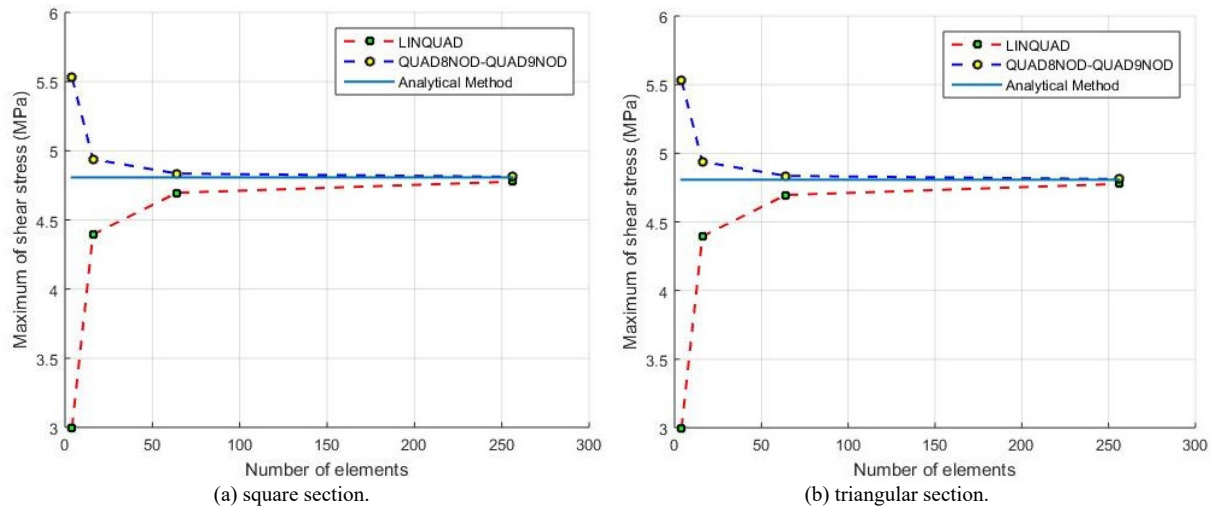(a) square section.   (b) triangular section.

Fig. 4: The values of maximum shear stress of three elements with respect to the number of elements for (a) square section and (b) triangular section.
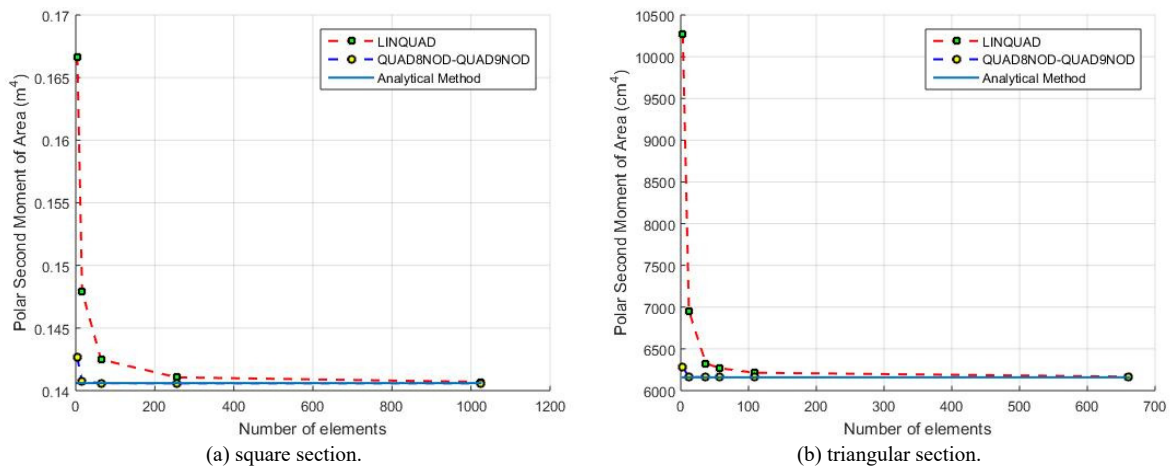
(a) square section.   (b) triangular section.

Fig. 5:   The Polar Second Moment of Area correspond with respect to the number of elements for square section (a) and triangular section (b).
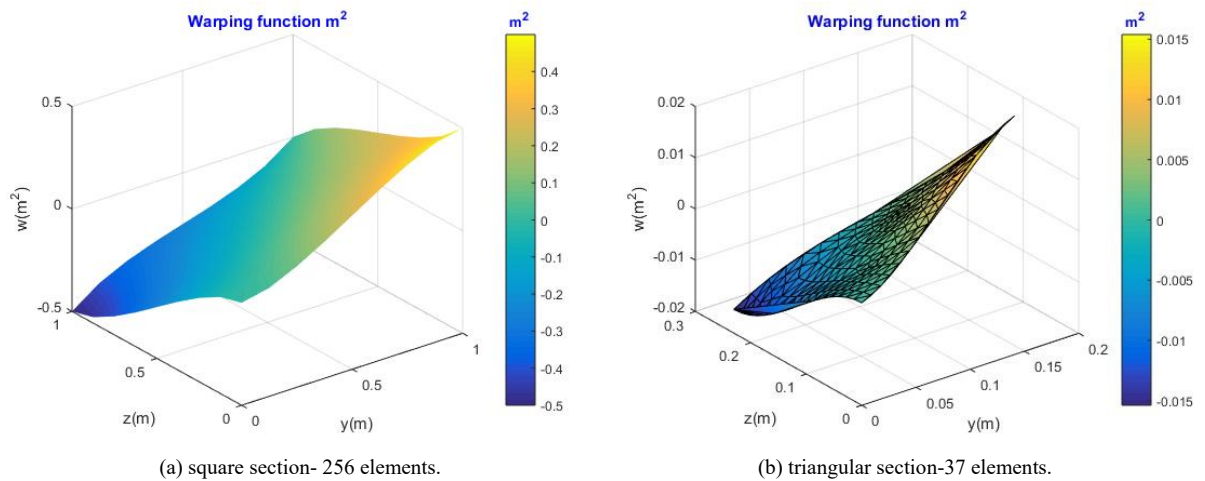

(a) square section- 256 elements.   (b) triangular section-37 elements.

Fig. 6:   Computed warping function for torsion ω^T for square section with 256 elements (a) and triangular section with 37 elements (b).
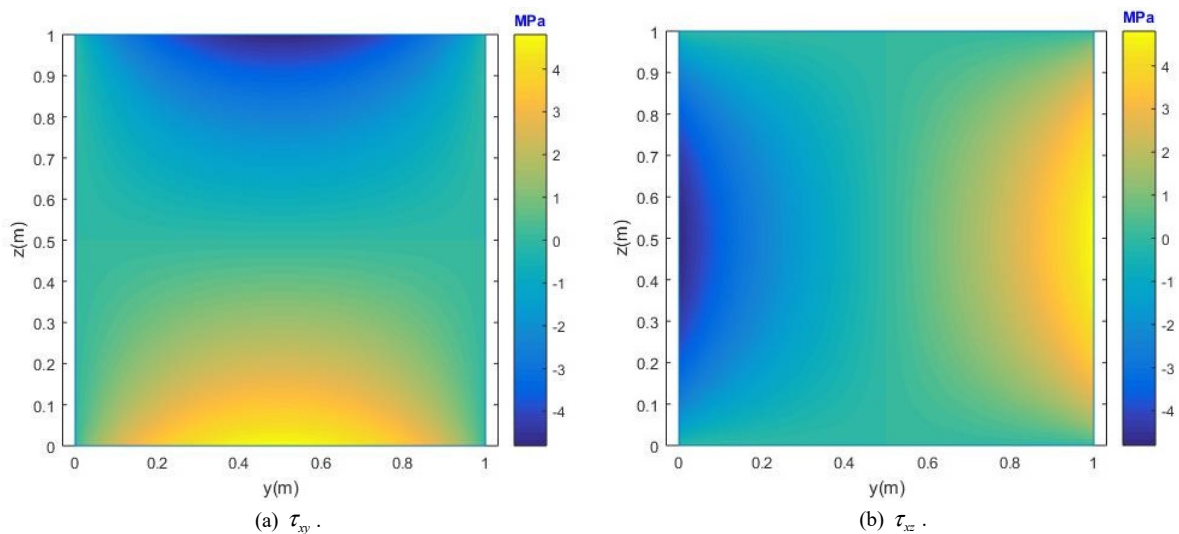

(a) τ_{xy} .   (b) τ_{xz} .

Fig. 7:   Computed shear stresses τ_{xy} (a) and τ_{xz} (b) for square section.

(a) τ_{xy} (b) τ_{xz}
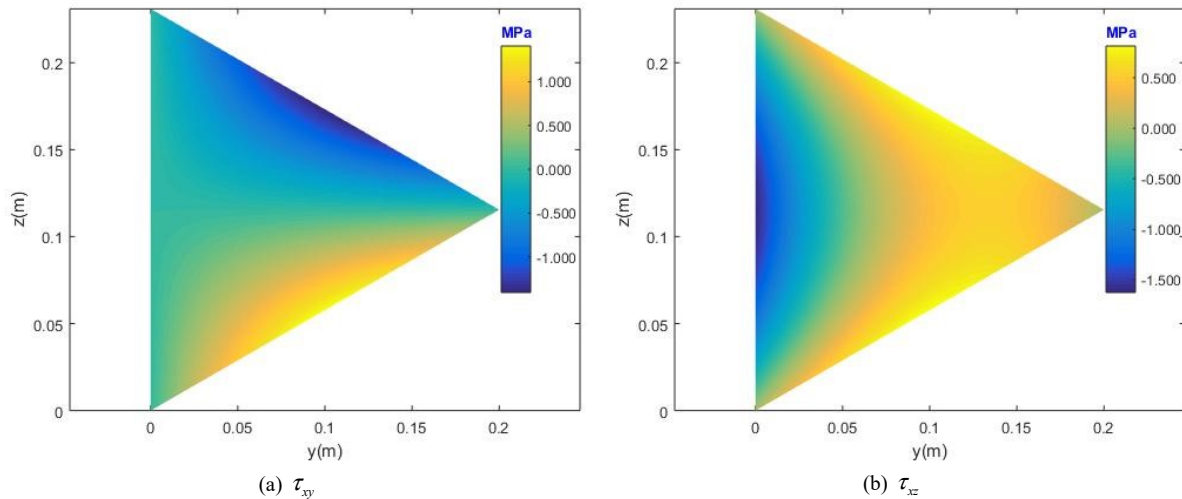
Fig. 8: Computed shear stresses τ_{xy} (a) and τ_{xz} (b) for triangular section.

References

[1] Timoshenko, Stephen, S. Timoshenko, and J. N. Goodier. *Theory of Elasticity*, by S. Timoshenko and JN Goodier,... McGraw-Hill book Company, 1951.

[2] Gruttmann, F., R. Sauer, and W. Wagner. "Shear stresses in prismatic beams with arbitrary cross-sections." *International journal for numerical methods in engineering* 45.7 (1999): 865-889.

[3] Zienkiewicz, Olek C., Robert L. Taylor, and Jian Z. Zhu. *The finite element method: its basis and fundamentals*. Elsevier, 2005.

[4] Reddaiah, P. "Deriving shape functions for 9-noded rectangular element by using lagrange functions in natural coordinate system and verified." *International Journal of Mathematics Trends and Technology* (IJMTT) 51.6 (2017).

About Authors

Dang-Bao TRAN was born in Dong Nai Province, Vietnam. He received his M.Sc. from Ho Chi Minh University of Technology (Vietnam) in 2009. He is currently with Thu Dau Mot University in Vietnam as a lecturer and with VSB–Technical University of Ostrava as a Ph.D. Student in Theory of Construction of Faculty of Civil Engineering. His research interests include Reinforced Concrete, Prestressed Concrete, Finite Element Method.

Assoc. Prof. Jaroslav NAVRÁTIL, M.Sc., Ph.D. Jaroslav Navrátil is recognized expert in the field of concrete and prestressed concrete structures, chartered engineer in statics and dynamics of structures and forensic expert in civil engineering. His professional focus is the development of computational methods for the design and analysis of structures and their implementation in a form of algorithms and computer programs. He has more than twenty years of experience in leading software development for design of reinforced and prestressed concrete structures and managing customer projects. Jaroslav Navrátil works as associate professor at VSB–Technical University of Ostrava and as development manager in Allplan Infrastructure.

Martin ČERMÁK was born in Hranice, Czech Republic. He received his M.Sc. in Computational Mathematics in 2008. He finished PhD. in 2012 in Computational Mathematics and reached the position of Associate Professor in 2018 at VSB–Technical University of Ostrava. Since 2018, he is Head of the Department of Mathematics at Faculty of Civil Engineering, VSB–TUO. His research interests include scalable algorithms for solving elastoplastic problems, material nonlinearities, contact problems, quadratic programming, non-overlapping domain decomposition, and parallel implementation of these methods.

Appendix A

This appendix completes Section 2 with the shape function of finite elements

A1. *LINQUAD* element

The reference *LINQUAD* element is defined on a rectangle with 4 nodes with coordinates:

$$M_1 = [-1,-1], \quad M_2 = [-1,1], \quad M_3 = [1,1], \quad M_4 = [-1,1],$$

and 4 corresponding linear shape function:

$$N_1(x,h) = \frac{1}{4}(1-x)(1-h), \quad N_2(x,h) = \frac{1}{4}(1+x)(1-h),$$

$N_3(x,h) = \frac{1}{4}(1+x)(1-h)$, $N_4(x,h) = \frac{1}{4}(1-x)(1+h)$.

A2. *QUAD8NOD* element

The reference *QUAD8NOD* element is defined on a rectangle with 8 nodes with coordinates:

$M_1 = [-1,-1]$, $M_2 = [-1,1]$, $M_3 = [1,1]$, $M_4 = [-1,1]$,

$M_5 = [0,-1]$, $M_6 = [1,0]$, $M_7 = [0,1]$, $M_8 = [-1,0]$,

and 8 corresponding shape function:

$N_1(x,h) = \frac{1}{4}(1-x)(1-h)(-1-x-h)$,

$N_2(x,h) = \frac{1}{4}(1+x)(1-h)(-1+x-h)$,

$N_3(x,h) = \frac{1}{4}(1+x)(1-h)(-1+x+h)$,

$N_4(x,h) = \frac{1}{4}(1-x)(1+h)(-1+x+h)$,

$N_5(x,h) = \frac{1}{2}(1-x^2)(1-h)$,

$N_6(x,h) = \frac{1}{2}(1+x)(1-h^2)$,

$N_7(x,h) = \frac{1}{2}(1-x^2)(1+h)$,

$N_8(x,h) = \frac{1}{2}(1-x)(1-h^2)$.

A3. *QUAD9NOD* element

The reference *QUAD9NOD* element is defined on a rectangle with 9 nodes with coordinates:

$M_1 = [-1,-1]$, $M_2 = [-1,1]$, $M_3 = [1,1]$, $M_4 = [-1,1]$,

$M_5 = [0,-1]$, $M_6 = [1,0]$, $M_7 = [0,1]$, $M_8 = [-1,0]$,

$M_9 = [0,0]$,

and 9 corresponding shape function:

$N_1(x,h) = \frac{x(x-1)h(h-1)}{4}$,

$N_2(x,h) = \frac{(x+1)xh(h-1)}{4}$,

$N_3(x,h) = \frac{(x+1)x(h+1)h}{4}$,

$N_4(x,h) = \frac{x(x-1)(h+1)h}{4}$,

$N_5(x,h) = \frac{(x+1)(x-1)h(h-1)}{-2}$,

$N_6(x,h) = \frac{(x+1)x(h+1)(h-1)}{-2}$,

$N_7(x,h) = \frac{(x+1)(x-1)(h+1)h}{-2}$,

$N_8(x,h) = \frac{x(x-1)(h+1)(h-1)}{-2}$,

$N_9(x,h) = \frac{(x+1)(x-1)(h+1)(h-1)}{1}$.